Supporting Information

Combined Effects of Functional Groups, Lattice Defects, and Edges in the Infrared Spectra of Graphene Oxide

Cui Zhang,[†] *Daniel M. Dabbs,*[‡] *Li-Min Liu,*[†,§] *Ilhan A. Aksay,*[‡] *Roberto Car*[†] *and Annabella Selloni*[*,†]

[†]Department of Chemistry and [‡]Department of Chemical and Biological Engineering, Princeton University, Princeton, New Jersey 08544, United States

[§]Present address: Beijing Computational Science Research Center, Beijing 100084, China

*Address correspondence to aselloni@princeton.edu

Experiment: Sample preparation

The procedure for producing GO using a modified Hummers method[1] has been described previously[2] and is summarized here. In a typical procedure, 3 g of flake graphite (Asbury grade 3061, Asbury, NJ) and 18 g of $KMnO_4$ were slowly added to 400 mL of a stirred solution composed of 360 mL H_2SO_4 and 40 mL H_3PO_4. The oxidation was continued for ~16 h with the temperature of the reaction vessel held at 50 °C. After cooling, 6 mL of H_2O_2 was added to the stirring suspension with the color of the suspension changing from brown to bright yellow. The suspension was separated and put into two 500 mL centrifuge tubes, then centrifuged for 15 min at 1800 g (Centra GP8R centrifuge, IEC, Thermo Scientific). The supernatant was discarded and the sediment re-suspended in water. This washing procedure was repeated several times, first using 250 mL of 12N HCl (aq) followed by three to four washes using 250 mL of ethanol, until the residual chlorine content was observed to remain stable, determined by elemental analysis using energy dispersive X-ray spectroscopy (EDS) (INCAx-act, Oxford Instruments, Abingdon, UK). The $KMnO_4$, H_2SO_4, H_3PO_4, HCl (aq), and H_2O_2 used in the synthesis and washing of GO were all high purity and used without modification (Alfa-Aesar and Fisher Scientific, Pittsburgh, PA). The material used for spectral analysis (IR and EDS) was removed from ethanol suspension and spray dried (Portable spray dryer, Niro, Inc., Columbia, MD) to remove the solvent, eliminate adsorbed and/or entrained water, and to reduce aggregate size. The carbon-to-oxygen molar ratio of the GO produced by this method was typically 1.7-2.0, measured by EDS.

FGSs were produced through the simultaneous thermal exfoliation and reduction of graphite oxide as described previously.[3,4] Briefly, dry graphite oxide powder was placed at the sealed end of a fused silica tube (Technical Glass Products) and dried overnight under flowing nitrogen. The tube was evacuated and purged with ultrahigh-purity argon (Air Products) three times. A vacuum was again pulled on the tube and the sealed end quickly inserted into a three-zone tube furnace

(Lindberg/Blue M, SPX Thermal Product Solutions) at 1100 ° C, and held there for 60 s to separate the graphite oxide into single sheets.[3] The as-produced FGS powder was black, with a typical surface area of ~ 690 $m^2 \cdot g^{-1}$, measured using nitrogen adsorption (Gemini V, Micrometrics Instruments Corporation) by the Brunauer, Emmett, and Teller (BET) method.[5]. Further reduction of the FGSs was done by leaving the FGSs in the tube furnace for longer periods, or by subsequently annealing the FGSs in a high temperature graphite-element furnace (Astro1000, Thermal Technologies) under argon for one hour.[6] The C/O of the resulting FGS powders was determined by combustion analysis (Atlantic Microlabs, Norcross, GA) and EDS. For the FGS heated to 1100 °C, the measured C/O was ~ 83.

Experiment: DRIFTS Spectra of GO and FGS

DRIFTS is a technique that better addresses the many physical limitations in charting the infrared absorbance of high carbon-content materials,[7] while offering a sensitive method for identifying oxygen functionalities on the carbon surface.[8,9] The high oxygen content of GO yields comparatively strong reflectance bands, but its IR spectrum is complicated by the presence of physisorbed water molecules held between the layers of graphene oxide sheets.[10,11] Since the FGS samples are produced by drying from suspension, aggregation of the sheets on the sample holder occurs, and sheets form overlapping stacks. Our model does not account for the effect of stacking.

Thermally exfoliating GO to create FGS removes some of the excess water, but the process simultaneously reduces the graphene oxide, increasing the C/O[12,13] and the number of defects[14,15] within the sheets.[14,15] Although the thermally reduced FGS is hydrophobic, water molecules will interact with the remaining oxygen groups, and physisorbed water is always apparent in samples. Generally, weaker IR absorption results from the decrease in the number of oxygen-containing

functional groups, and spectral resolution is further diminished by an increase in the broad spectrum absorptivity of the carbonaceous material.[8]

A method used to produce graphene oxide with lower defect content than that produced by the modified Hummers technique[16] indicates that the reduction in defect content has little effect on band position, and primarily changes the intensity of the absorbance bands related to carbonyls (1735 cm^{-1}), adsorbed water (1625 cm^{-1}), and sp^2 carbon-carbon bonds (1580 cm^{-1}).[16] The same broad effect is seen in our system: increasing the defect density by thermal reduction has little discernible effect on the positions of the three bands at 1740 cm^{-1}, 1615 cm^{-1}, and 1584 cm^{-1}, although the relative intensities of the bands change dramatically with reduction. The reduction in the carbonyl band intensity (1740 cm^{-1}) is easily understood as due to the thermal reduction, but the changes in band intensity exhibited by the supposed water adsorption and carbon-carbon double band are not so simply explained. Also significant, two well-defined absorption bands appear in the thermally reduced FGS at 1511 and 1454 cm^{-1}, structures that have been previously observed to form during thermal annealing (albeit at much lower temperatures).[17]

Despite the loss of oxygen, the sensitivity of DRIFTS in detecting the remaining oxygen-containing functional groups is high enough that the respective absorption bands are sharper and better separated in the IR spectrum for the FGS than in the GO spectrum.[10] The C/O of FGS can be raised by one or two orders of magnitude above that of the GO through a combination of exfoliation temperature and subsequent heating at high temperature under argon.[6] If the subsequent heating temperature is kept below 1200 °C, the C/O can be raised[6] to near 100 with the defect content also increasing with increasing temperature.[14] Existing defects do not heal by annealing out of the lattice[6,18] nor does the degree of sp^2 in the lattice change significantly until the temperature of the material is raised above 1200 °C.[19-20] Heating the FGS to 1100 °C helps to define the oxygen

groups on the graphene oxide sheet by reducing near neighbor effects and raises the defect content of the FGS, increasing the visibility of interactions between vacancies and the functional groups.

Computational Details: Vibrational Density of States

Vibrational density of states (VDOS) were calculated from *ab initio* molecular dynamics (AIMD) simulations via the Fourier transform of the velocity-velocity autocorrelation function of each atomic species.[21] This allowed us to obtain an independent identification of the partial contributions of each atomic species to the vibrational modes. Vibrational frequencies obtained from AIMD are red shifted with respect to those given by DFPT for two reasons. One is anharmonicity, included in finite temperature MD simulations, and the other is our choice for the fictitious electron mass in Car-Parrinello simulations. The adopted value (300 au) is a compromise between accuracy and numerical efficiency. A smaller value would improve the accuracy of the calculated frequencies, particularly those involving H stretching modes, at the expense of an increase in the computational cost.

Table S1: Infrared peak assignments for carbon oxides in oxidized carbon black.[22]

Group or functionality	**Assignment regions (cm^{-1})**		
C-O stretch of ethers	1000-1300		
Ether bridge	1230-1250		
Cyclic ethers	1025-1141		
Alcohols	1049-1276		3200-3640
Phenols: C-OH stretch	1000-1220		
Phenols: O-H bend & stretch	1160-1200		2500-3620
Aromatic C=C stretch (activated)	1590-1600		
Quinones	1550-1680		
Carboxylic acids	1120-1200	1665-1760;	2500-3300
Lactones	1160-1370	1675-1790	
Anhydrides	980-1300	1740-1880	
Ketenes			2080-2200
C-H stretch			2600-3000

Table S2: Infrared peak assignments for GO and graphene oxides, from literature.

Group or functionality	**Frequency (cm^{-1})**	**References**
Unassigned	828	23
Epoxide bending	800-900	17, 24
C-O skeletal mode	968	23
Ethers and/or epoxides	1000-1280	16, 25
	1280-1320	16, 17, 24
C-C skeletal mode	1064	10, 16, 23
C-OH	1070	24
C-OH, carboxyl	1080	24
C-OH	1368, 1370	10, 23
Aromatic C=C (activated)	1500-1600	7, 10, 16, 17, 23, 24
H_2O	1616, 1628	10, 16, 23, 26
Carboxyls and/or H_2O	1600-1750	17
Carboxyls	1650-1750	25
Ketones	1650-1700	7
Carboxyls	1740-1750	7
Lactones	1790	7
C=O, ketones	1714-1850	10, 16, 17, 23, 25
Dimeric COOH	2814, 2780	10, 23
H_2O	3210, 3190	10, 23
C-OH, carboxyl	3490	10, 23, 24
C-OH	3630	10, 23
	3050-3800	24
-OH (ads. H_2O and -OH)	3200-3800	10, 16, 23, 25

Table S3: Comparison between computed and experimental IR frequencies (cm^{-1}) of gas phase carbon monoxide, carbon dioxide, methane and water. Calculated frequencies are obtained with density functional perturbation theory.[a]

	CO	CO_2		CH_4		H_2O		
	ν	ν_b	ν_{as}	ν_b	ν_{as}	ν_b	ν_s	ν_{as}
Cal.	2124	649	2343	1309	3092	1598	3668	3781
Exp.	2170	677	2349	1306	3019	1595	3657	3756

[a] Cubic cell size 15 Å; Ecut = 80 Ry; ν:stretching frequency; ν_b: bending frequency; ν_{as}: asymmetric stretching frequency; ν_s: symmetric stretching frequency.

Table S4: Computed IR frequencies (cm^{-1}) for **Models I-IV**, compared to experimental DRIFTS data for GO and FGS after heating to 1100°C. Band assignments to specific functional groups in the computed spectra are based on the normal mode analysis. Weak spectral features or shoulders are denoted as '(sh)'.

Group or Functionality	**Model I**	**Model II**	**Model III**	**Model IV**	**GO, as prepared**	**FGS heated to 1100°C**
Overlapped regions	1012		1026 (sh)			1050
		1065		1074	1082	1072
	1110	1159	1129	1146 (sh)	1155	1182
-OH bend			1275	1216	1234	1242
	1331	1319		1307		1302
			1337	1375	1366	1361
	1400	1423	1417			1454
C-H (edge)			1555			
C=C		1607		1601	1584	1511, 1583
H_2O					1615	1611
C=O (vac)		1664		1664		
C=O (edge)			1715	1718		
C=O carboxyl					1740	1732
-OH carboxyl			1784			
C=O (edge) lactone				1812		
			1959			
						2780-3000
-OH str.			3118			
	3279		3195	3205		
	3364	3374	3308			3365
	3473	3430	3444	3475	3436	3428
		3550	3532	3587		
	3606		3633		3626	3675
			3898			

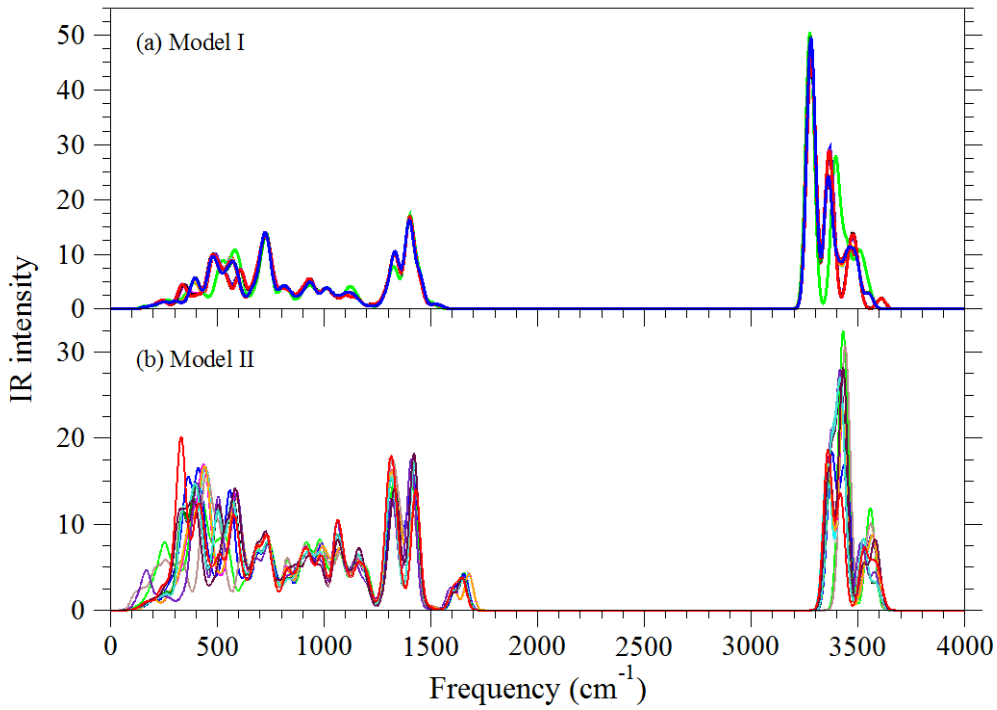

Figure S1: IR spectra of all 18 snapshots at time intervals of 2.3 ps from each 41-ps MD trajectory of (a) extended graphene oxide defect free (**Model I**) and (b) extended graphene oxide with monovacancy (**Model II**).

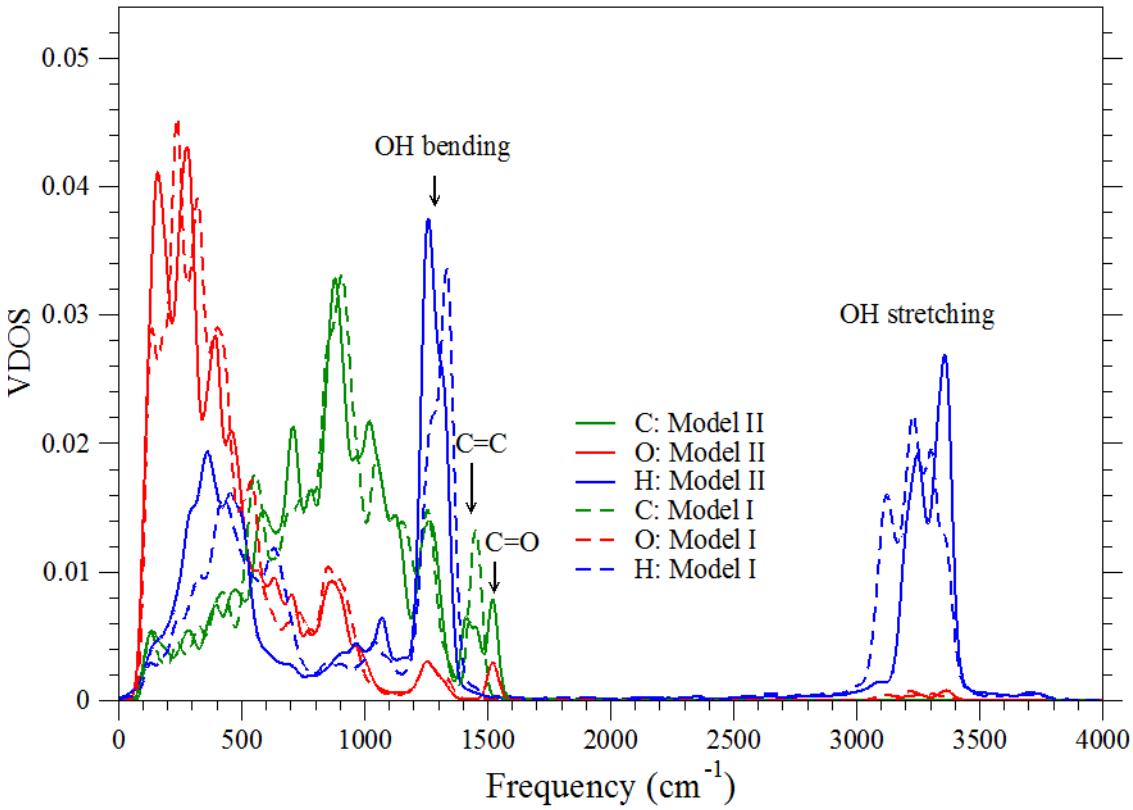

Figure S2: Vibrational density of states (VDOS) of carbon (green), oxygen (red) and hydrogen (blue) atoms in **Model I** (dashed line) and **Model II** (solid line).

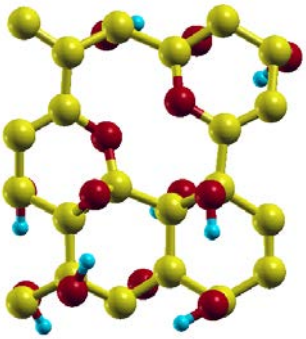

(a) **Model IIb**

(b) **Model IVb**

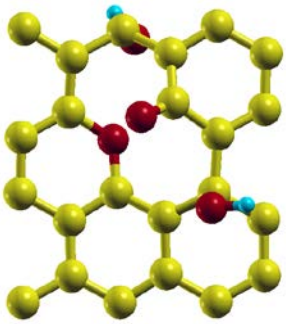

(c) **Model V**

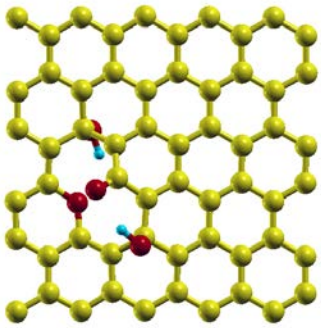

(d) **Model VI**

Figure S3: Atomic structure of graphene oxide models. (a) extended graphene oxide with divacancy and a C/O of 1.69 (**Model IIb**); (b) finite graphene oxide with monovacancy and a C/O of 2 (**Model IVb**); (c) extended reduced graphene oxide with monovacancy and a C/O of ~ 6 (**Model V**); (d) extended reduced graphene oxide with monovacancy and a C/O of ~ 15 (**Model VI**). **Model IIb** is constructed by removing one more carbon atom at the monovacancy of **Model II** and saturating the divacancy with two ether groups. **Model IVb** is derived from finite graphene oxide **Model IV** by adding a monovacancy decorated with ketone and ether groups in the middle of graphene sheet. Reduced graphene oxide **Models V** and **VI** contain the same type of monovacancy but different numbers of lattice points (24 and 60, respectively) in the unit cells, leading to different C/O.

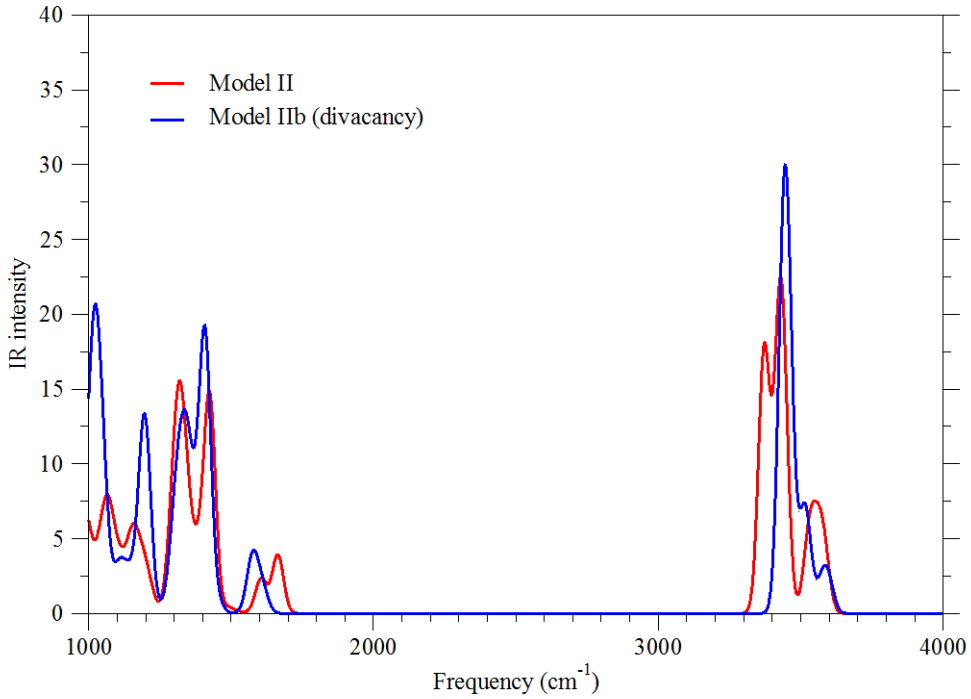

Figure S4: Comparison between the IR spectra of extended graphene oxide with a monovacancy and a C/O of 1.64 (**Model II**, red) and with a divacancy and a C/O of 1.69 (**Model IIb**, blue).

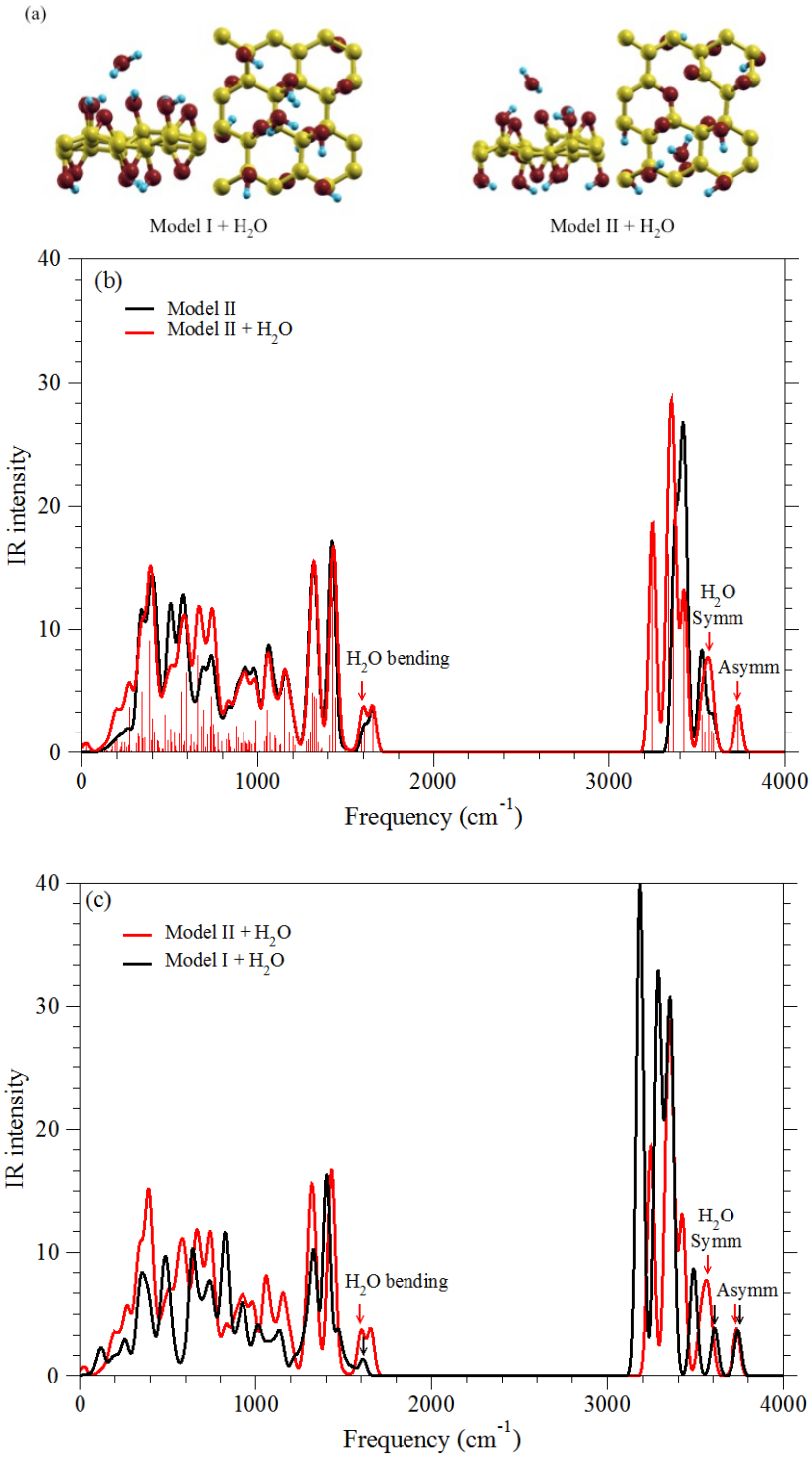

Figure S5: (a) Side and top views of the optimized structures of **Models I** and **II** with an adsorbed water molecule. (b) IR spectra of **Model II** with and without an adsorbed water molecule. (c) Comparison of the IR spectra of **Models I** and **II,** each with an adsorbed water molecule**.**

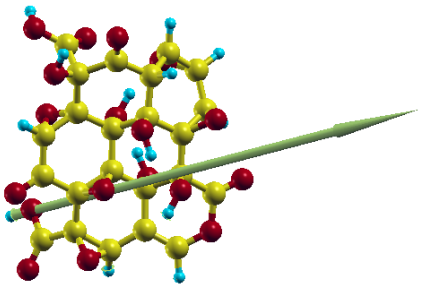

(a) Carboxyl OH stretching (3879 cm^{-1})

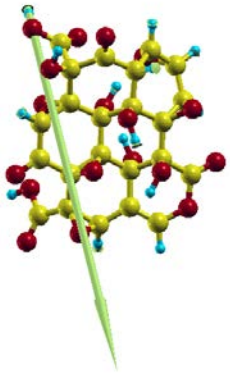

(b) Carboxyl OH stretching (3196 cm^{-1})

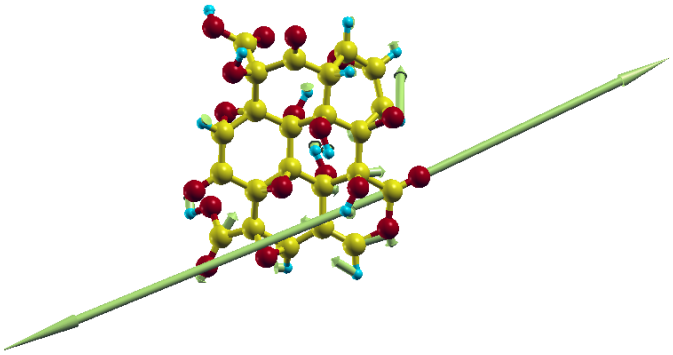

(c) Lactone C=O stretching (1799 cm^{-1})

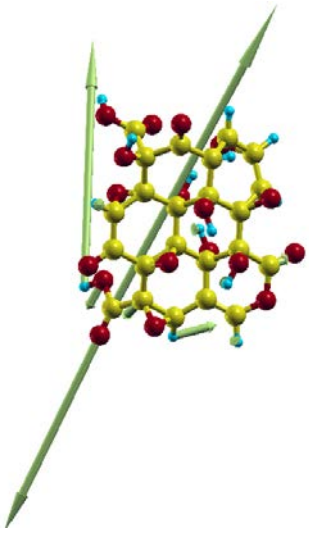

(d) A combination mode of carboxyl OH bending and C=O stretching (1781 cm^{-1})

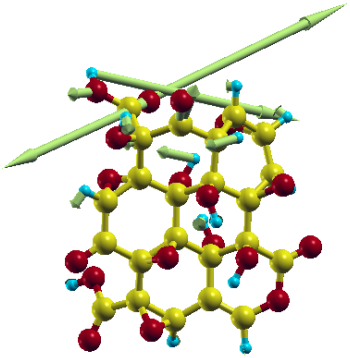

(e) A combination mode of carboxyl OH bending and C=O stretching (1749 cm^{-1})

Figure S6: Vibrational normal modes of the finite graphene oxide **Model III**.

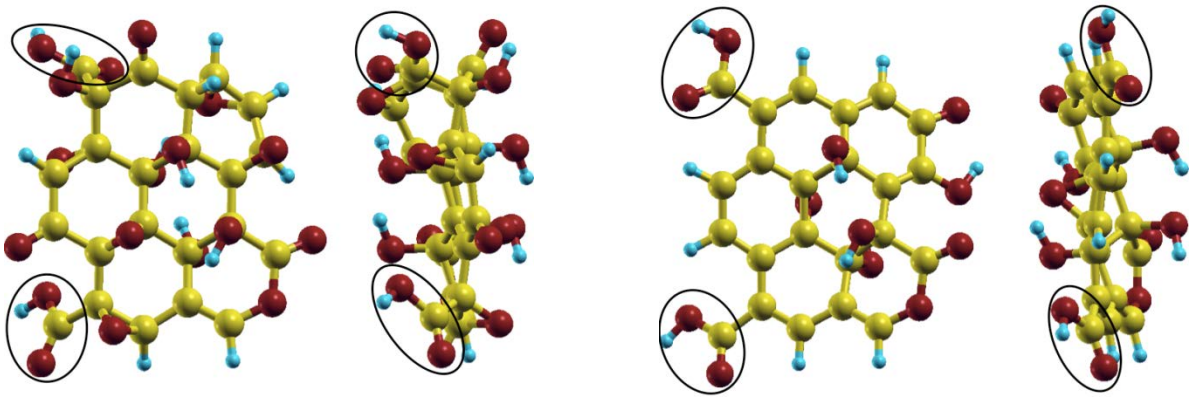

(a) Model III: top (left) and side (right) views (b) Model IV: top (left) and side (right) views

Figure S7: Optimized structures of the finite graphene oxide **Models III** (a) and **IV** (b). Orientations of carboxyl groups with respect to the graphene oxide plane are highlighted with black circles.

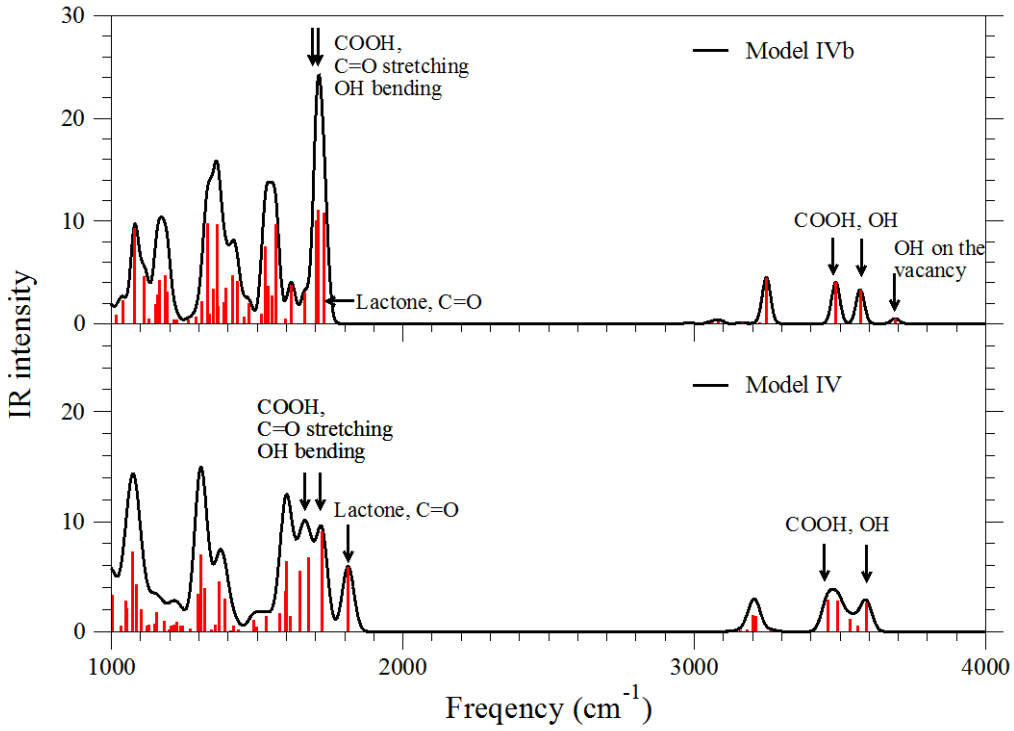

Figure S8: Comparison between the IR spectra of finite graphene oxide **Model IVb** with monovacancy and a C/O of 2 (upper panel) and **Model IV** with a C/O of 1.92 (lower panel, also see Figure 5(b)).

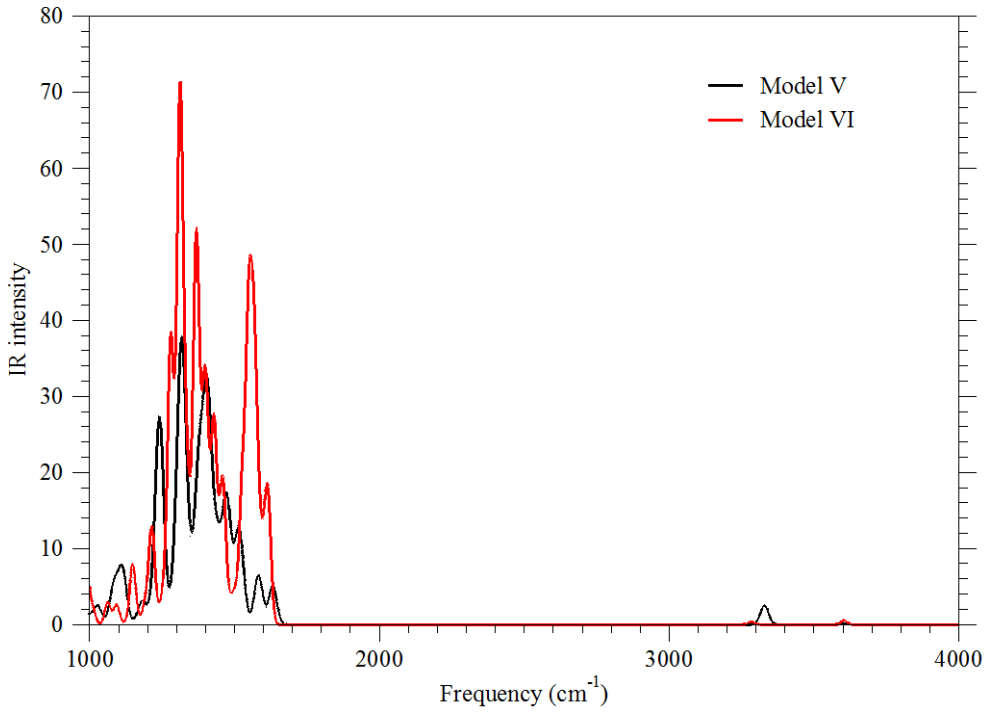

Figure S9: Comparison between the IR spectra of extended graphene oxide **Models V** and **VI**. **Model V** includes a monovacancy every 24 lattice points leading to a C/O of ~ 6 and **Model VI** comprises a monovacancy every 60 lattice points yielding a C/O of ~ 15.

References

1. Marcano, D. C.; Kosynkin, D. V.; Berlin, J. M.; Sinitskii, A.; Sun, Z. Z.; Slesarev, A.; Alemany, L. B.; Lu, W.; Tour, J. M., Improved synthesis of graphene oxide. *ACS Nano* **2010**, *4*, 4806-4814.
2. Pope, M. A.; Korkut, S.; Punckt, C.; Aksay, I. A., Supercapacitor electrodes produced through evaporative consolidation of graphene oxide-water-ionic liquid gels. *J. Electrochem. Soc.* **2013**, *160*, A1653-A1660.
3. McAllister, M. J.; Li, J. L.; Adamson, D. H.; Schniepp, H. C.; Abdala, A. A.; Liu, J.; Herrera-Alonso, M.; Milius, D. L.; Car, R.; Prud'homme, R. K., *et al*., Single sheet functionalized graphene by oxidation and thermal expansion of graphite. *Chem. Mater.* **2007**, *19*, 4396-4404.
4. Hsieh, A. G.; Korkut, S.; Punckt, C.; Aksay, I. A., Dispersion stability of functionalized graphene in aqueous sodium dodecyl sulfate solutions. *Langmuir* **2013**, *29*, 14831-14838.
5. Brunauer, S.; Emmett, P. H.; Teller, E., Adsorption of gases in multimolecular layers. *J. Am. Chem. Soc.* **1938**, *60*, 309-319.
6. Punckt, C.; Muckel, F.; Wolff, S.; Aksay, I. A.; Chavarin, C. A.; Bacher, G.; Mertin, W., The effect of degree of reduction on the electrical properties of functionalized graphene sheets. *Appl. Phys. Lett.* **2013**, *102*, 023114-5.
7. Fuente, E.; Menéndez, J. A.; Díez, M. A.; Suárez, D.; Montes-Morán, M. A., Infrared spectroscopy of carbon materials: a quantum chemical study of model compounds. *J. Phys. Chem. B* **2003**, *107*, 6350-6359.
8. Venter, J. J.; Vannice, M. A., A Diffuse reflectance FTIR spectroscopic (DRIFTS) investigation of carbon-supported metal-carbonyl clusters. *J. Am. Chem. Soc.* **1987**, *109*, 6204-6205.
9. Venter, J. J.; Vannice, M. A., Applicability of DRIFTS for the characterization of carbon-supported metal-catalysts and carbon surfaces. *Carbon* **1988**, *26*, 889-902.
10. Szabó, T.; Berkesi, O.; Dékány, I., DRIFT study of deuterium-exchanged graphite oxide. *Carbon* **2005**, *43*, 3186-3189.
11. Acik, M.; Mattevi, C.; Gong, C.; Lee, G.; Cho, K.; Chhowalla, M.; Chabal, Y. J., The role of intercalated water in multilayered graphene oxide. *ACS Nano* **2010**, *4*, 5861-5868.
12. McAllister, M. J.; Li, J. L.; Adamson, D. H.; Schniepp, H. C.; Abdala, A. A.; Liu, J.; Herrera-Alonso, M.; Milius, D. L.; Car, R.; Prud'homme, R. K., et al., Single sheet functionalized graphene by oxidation and thermal expansion of graphite. *Chem. Mater.* **2007**, *19*, 4396-4404.
13. Schniepp, H. C.; Li, J. L.; McAllister, M. J.; Sai, H.; Herrera-Alonso, M.; Adamson, D. H.; Prud'homme, R. K.; Car, R.; Saville, D. A.; Aksay, I. A., Functionalized single graphene sheets derived from splitting graphite oxide. *J. Phys. Chem. B* **2006**, *110*, 8535-8539.
14. Korkut, S.; Ozbas, B.; Milius, D. L.; Liu, J.; Aksay, I. A., Effect of high temperature annealing on the structure of functionalized graphene sheets princeton university: Submitted, 2014.
15. Eigler, S.; Dotzer, C.; Hirsch, A.; Enzelberger, M.; Müller, P., Formation and decomposition of CO_2 intercalated graphene oxide. *Chem. Mater.* **2012**, *24*, 1276-1282.
16. Eigler, S.; Enzelberger-Heim, M.; Grimm, S.; Hofmann, P.; Kroener, W.; Geworski, A.; Dotzer, C.; Röckert, M.; Xiao, J.; Papp, C., et al., Wet chemical synthesis of graphene. *Adv. Mater.* **2013**, *25*, 3583-3587.
17. Acik, M.; Lee, G.; Mattevi, C.; Pirkle, A.; Wallace, R. M.; Chhowalla, M.; Cho, K.; Chabal, Y., The role of oxygen during thermal reduction of graphene oxide studied by infrared absorption spectroscopy. *J. Phys. Chem. C* **2011**, *115*, 19761-19781.

18. Campos-Delgado, J.; Kim, Y. A.; Hayashi, T.; Morelos-Gomez, A.; Hofmann, M.; Muramatsu, H.; Endo, M.; Terrones, H.; Shull, R. D.; Dresselhaus, M. S., et al., Thermal stability studies of cvd-grown graphene nanoribbons: defect annealing and loop formation. *Chem. Phys. Lett.* **2009**, *469*, 177-182.
19. Emmerich, F. G., Evolution with heat treatment of crystallinity in carbons. *Carbon* **1995**, *33*, 1709-1715.
20. Oberlin, A., Carbonization and graphitization. *Carbon* **1984**, *22*, 521-541.
21. Rahman, A., Correlations in the motion of atoms in liquid argon. *Phys. Rev.* **1964**, *136*, A405-A411.
22. Fanning, P. E.; Vannice, M. A., A DRIFTS study of the formation of surface groups on carbon by oxidation. *Carbon* **1993**, *31*, 721-730.
23. Szabo, T.; Berkesi, O.; Forgo, P.; Josepovits, K.; Sanakis, Y.; Petridis, D.; Dekany, I., Evolution of surface functional groups in a series of progressively oxidized graphite oxides. *Chem. Mater.* **2006**, *18*, 2740-2749.
24. Acik, M.; Lee, G.; Mattevi, C.; Chhowalla, M.; Cho, K.; Chabal, Y. J., Unusual infrared-absorption mechanism in thermally reduced graphene oxide. *Nat. Mater.* **2010**, *9*, 840-845.
25. Bagri, A.; Mattevi, C.; Acik, M.; Chabal, Y. J.; Chhowalla, M.; Shenoy, V. B., Structural evolution during the reduction of chemically derived graphene oxide. *Nat. Chem.* **2010**, *2*, 581-587.
26. Dimiev, A. M.; Alemany, L. B.; Tour, J. M., Graphene oxide. origin of acidity, its instability in water, and a new dynamic structural model. *ACS Nano* **2013**, *7*, 576-588.